Endothelial nitric oxide synthase regulates N-Ras activation on the Golgi complex of antigen-stimulated T cells

Sales Ibiza*, Andrea Pérez-Rodríguez†, Ángel Ortega‡, Antonio Martínez-Ruiz§, Olga Barreiro*§, Carlota A. García-Domínguez†, Víctor M. Víctor¶, Juan V. Esplugues‖, José M. Rojas†, Francisco Sánchez-Madrid*§, and Juan M. Serrador*,**

*Departamento de Biología Vascular e Inflamación, Centro Nacional de Investigaciones Cardiovasculares, E-28029 Madrid, Spain; †Unidad de Biología Celular, Centro Nacional de Microbiología, Majadahonda, E-28220 Madrid, Spain; ‡Unidad Central de Investigación Medicina, Facultad de Medicina, and ‖Departamento de Farmacología and Ciberehd, Universitat de Valencia, E-46010 Valencia, Spain; §Servicio de Inmunología, Hospital de la Princesa, Universidad Autónoma de Madrid, E-28006 Madrid, Spain; and ¶Fundación Hospital Universitario Doctor Peset, E-46017 Valencia, Spain

Edited by Jonathan S. Stamler, Duke University Medical Center, Durham, NC, and accepted by the Editorial Board May 20, 2008 (received for review November 21, 2007)

Ras/ERK signaling plays an important role in T cell activation and development. We recently reported that endothelial nitric oxide synthase (eNOS)-derived NO regulates T cell receptor (TCR)-dependent ERK activation by a cGMP-independent mechanism. Here, we explore the mechanisms through which eNOS exerts this regulation. We have found that eNOS-derived NO positively regulates Ras/ERK activation in T cells stimulated with antigen on antigen-presenting cells (APCs). Intracellular activation of N-, H-, and K-Ras was monitored with fluorescent probes in T cells stably transfected with eNOS-GFP or its G2A point mutant, which is defective in activity and cellular localization. Using this system, we demonstrate that eNOS selectively activates N-Ras but not K-Ras on the Golgi complex of T cells engaged with APC, even though Ras isoforms are activated in response to NO from donors. We further show that activation of N-Ras involves eNOS-dependent *S*-nitrosylation on Cys^{118}, suggesting that upon TCR engagement, eNOS-derived NO directly activates N-Ras on the Golgi. Moreover, wild-type but not C118S N-Ras increased TCR-dependent apoptosis, suggesting that *S*-nitrosylation of Cys^{118} contributes to activation-induced T cell death. Our data define a signaling mechanism for the regulation of the Ras/ERK pathway based on the eNOS-dependent differential activation of N-Ras and K-Ras at specific cell compartments.

S-nitrosylation | eNOS | apoptosis

A role for nitric oxide (NO) has been reported as a regulator of T cell development and differentiation (1). Previous studies have shown that human T cells produce NO and express endothelial nitric oxide synthase (eNOS) (2–4). eNOS is activated in a Ca^{2+}-dependent manner by the phosphoinositide 3-kinase (PI3K)/Akt pathway through the phosphorylation of Ser^{1179} (5, 6). eNOS activation also entails denitrosylation of eNOS, which is constitutively *S*-nitrosylated (7, 8). Another level of regulation is provided by posttranslational NH_2-terminal acylations, which determine eNOS subcellular localization: palmitoylation of Cys^{15} and Cys^{26} specifically targets eNOS to the plasma membrane, whereas myristoylation of Gly^2 provides the general membrane association required for *S*-nitrosylation and localization on the Golgi apparatus (7, 9). In T lymphocytes, Golgi-localized eNOS is activated in response to the binding of T cell receptor (TCR) to antigen on antigen-presenting cells (APCs) (10).

The actions of NO on T cells can occur through cGMP-dependent and -independent mechanisms. Prominent among cGMP-independent mechanisms is the activation of ERK mitogen-activated protein kinases (MAPKs) via the regulation of Ras activity (11, 12). Ras proteins are small GTPases implicated in T cell activation, proliferation, and apoptosis (13). Engagement of the TCR by CD3 Ab, superantigens, or antigenic peptides results in transient activation of Ras from the inactive GDP-bound state to the GTP-bound form (14). This GDP–GTP exchange is positively controlled by guanine nucleotide exchange factors (GEFs) such as RasGRP1 and is reversed by GTPase-activating proteins (GAPs), which stimulate the intrinsic GTPase activity of Ras.

T lymphocytes predominantly express N- and K-Ras, with very low levels of H-Ras (15). The three Ras isoforms share substantial homology, but they differ considerably in their C-terminal hypervariable regions, which determine their subcellular localization as a result of posttranslational acylations (16). Reversible palmitoylation of H-Ras and N-Ras on Cys^{181} allows their cycling between the plasma membrane and the Golgi apparatus, whereas the most frequent variant of K-Ras (K-Ras4B) contains a polybasic region that confines it to the plasma membrane (17). Recruitment of Raf-1 by GTP-bound Ras has generally been considered to take place at the plasma membrane before ERK activation (18); however, it has recently been shown that Ras activation can also occur on the Golgi apparatus (16). The pathway by which Golgi-associated Ras becomes activated involves PLC-γ and RasGRP1 (19). Moreover, previous studies in Jurkat cells suggest that Ras may be differentially activated in response to TCR stimulation (15). Despite these differences in localization and function, the mechanisms through which the different Ras isoforms become activated in membrane compartments are still poorly understood.

Here, we have investigated whether eNOS regulates the activation of Ras in antigen-stimulated T cells and the mechanisms that underlie this regulation. Our results show that N-Ras, but not K-Ras, is selectively activated by eNOS on the Golgi. Through a combination of affinity binding, quantitative confocal microscopy, and nitrosothiol (SNO) detection analyses, we further show that during antigen-specific T cell–APC interactions eNOS-derived NO activates Golgi-localized N-Ras by a mechanism identified with *S*-nitrosylation of Cys^{118}.

Results

eNOS Regulates Ras/ERK Signaling in Antigen-Specific T Cell–APC Conjugates. To study the mechanism by which NO regulates the activity of ERK in antigen-specific T cell–APC conjugates, we stably transfected hemagglutinin (HA)-specific TCR-V_β3-

Author contributions: J.M.S. designed research; S.I., A.O., A.M.-R., O.B., and V.M.V. performed research; A.P.-R., C.A.G.-D., and J.M.R. contributed new reagents/analytic tools; S.I., A.O., A.M.-R., V.M.V., and J.M.S. analyzed data; and S.I., J.V.E., F.S.-M., and J.M.S. wrote the paper.

The authors declare no conflict of interest.

This article is a PNAS Direct Submission. J.S.S. is a guest editor invited by the Editorial Board.

**To whom correspondence should be addressed. E-mail: jmserrador@cnic.es.

This article contains supporting information online at www.pnas.org/cgi/content/full/0711062105/DCSupplemental.

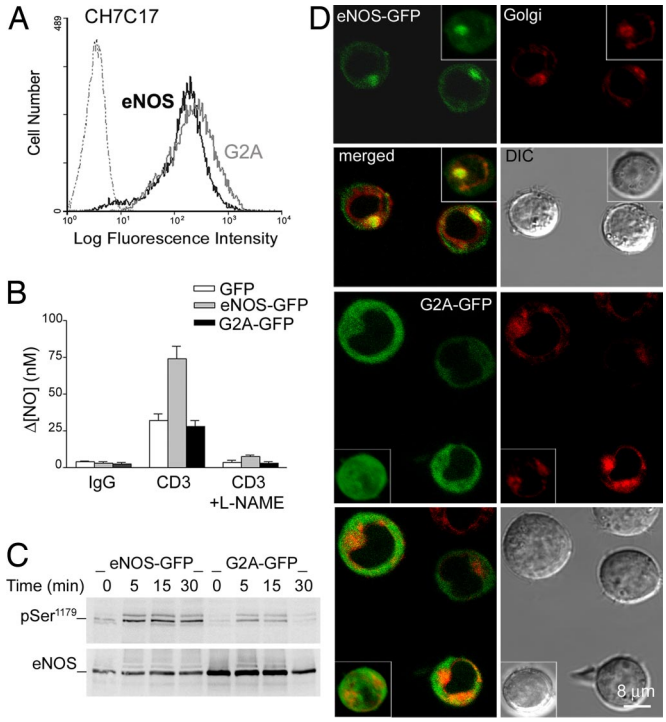

Fig. 1. NO production and eNOS expression, phosphorylation, and localization in eNOS- and G2A-GFP cells. (*A*) Flow cytometry of GFP fluorescence in CH7C17 T cells stably transfected with eNOS- or G2A-GFP. (*B*) Electrochemical detection of NO production in eNOS-, G2A-GFP, and control GFP cells stimulated for 30 min with CD3 Ab plus IgG cross-linking. For controls, cells were pretreated with the NOS inhibitor L-NAME (500 μM), or CD3 Ab was omitted (IgG). The means ± SEM of three independent experiments are shown. (*C*) Time course phosphorylation of eNOS- and G2A-GFP in cells stimulated with SEB-pulsed Raji APC for the times indicated. Phospho-Ser^{1179} and total eNOS- and G2A-GFP were detected by immunoblotting. A representative experiment of three is shown. (*D*) Confocal fluorescence microscopy and DIC images of live eNOS- and G2A-GFP cells labeled with the Golgi fluorescent probe Bodipy-TR ceramide. (*Insets*) Representative computerized 3D reconstructions of Golgi (red) and eNOS- or G2A-GFP (green).

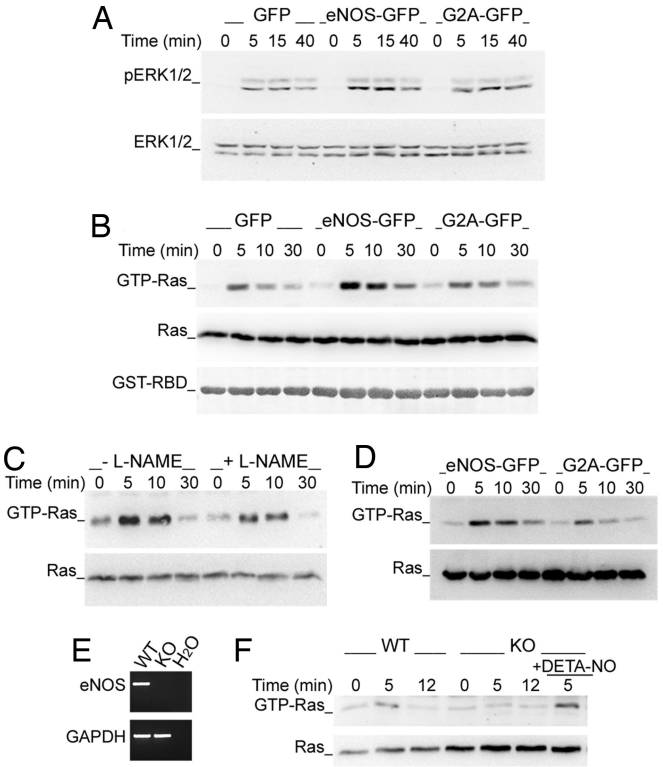

Fig. 2. eNOS increases the activation of Ras/ERK in T cells forming conjugates with antigen-pulsed APC. (*A* and *B*) GFP, eNOS-, and G2A-GFP cells were mixed with paraformaldehyde-fixed SEB-pulsed Raji cells for the times indicated. (*A*) Time course activation of ERK. (*B*) Time course activation of Ras determined by pull-down binding to GST-RBD-Raf-1 and subsequent immunoblotting with rabbit anti-pan-Ras mAb. GST-RBD-Raf-1 loadings are also shown. (*C*) Time course activation of Ras in eNOS-GFP cells pretreated with L-NAME or vehicle for 30 min before stimulation with SEB-pulsed Raji APC. (*D*) Time course activation of Ras in T cells conjugated with HA-pulsed HOM-2 cells. (*E*) RT-PCR of eNOS in T lymphoblasts from wild-type (WT) and eNOS-deficient (KO) mice. Control GAPDH mRNA expression is shown. (*F*) Ras activation in WT and eNOS KO mouse T lymphoblasts stimulated with CD3 Ab. As a control, eNOS KO cells were treated with 100 μM DETA-NO. Ras activation in *C*, *D*, and *F* was determined as in *B*. Each panel is representative of three independent experiments.

expressing CH7C17 T cells with a construct encoding eNOS fused at its C terminus to green fluorescent protein (eNOS-GFP) or with a similar construct encoding the eNOS G2A mutant (G2A-GFP). The altered subcellular positioning of this mutant renders it defective for NO synthesis (9, 20). The levels of eNOS- or G2A-GFP-expressed in cells were similar, as determined by flow cytometry (Fig. 1*A*). NOS activity was analyzed with an NO electrode. In response to TCR engagement, NO production in cells expressing eNOS-GFP was 2-fold higher than in GFP-expressing controls or G2A-GFP cells and was abrogated by pretreatment with the NOS inhibitor L-NAME (Fig. 1*B*).

The activation of eNOS- and G2A-GFP was studied in T cells forming conjugates with superantigen B (SEB)-pulsed Raji APCs. Phosphorylation on Ser^{1179} increased within 5 min of the initial T cell–APC contact and was markedly more pronounced in eNOS-GFP cells [Fig. 1*C* and supporting information (SI) Fig. S1]. To investigate eNOS and G2A intracellular localization, live or fixed cells were labeled with the Golgi-specific markers Bodipy Texas red ceramide or Golgin-97, respectively. The staining pattern of endogenous eNOS does not always fit exactly with that observed for eNOS-GFP because of their different expression levels and the antibodies used. Nonetheless, confocal fluorescence microscopy revealed that endogenous eNOS and eNOS-GFP both localized mainly on the Golgi complex, with a minor fraction at the plasma membrane, whereas the G2A mutant was distributed diffusely throughout the cytoplasm (Fig. 1*D* and Fig. S2).

To determine the involvement of the small GTPase Ras in eNOS-mediated ERK activation, extracts from serum-starved SEB-activated eNOS- or G2A-GFP cells were studied both by Western blotting with anti-phospho-ERK Abs and by pull-down with GST-linked Ras-binding domain of Raf-1 (GST-RBD-Raf-1). Activation of ERK was detected 5 min after the initial T cell–APC contact and diminished progressively from 15 min; Ras showed a similar but shorter-lived activation, and both were more strongly activated in eNOS-GFP than in either GFP or G2A-GFP T cells (Fig. 2 *A* and *B* and Fig. S3 *A* and B). Pretreatment of eNOS-GFP cells with L-NAME reduced Ras activation, confirming the dependence on eNOS (Fig. 2*C* and Fig. S3*C*). Ras activation was also stronger in eNOS-GFP cells stimulated with HA-pulsed HOM-2 APCs (Fig. 2*D* and Fig. S3*D*). To confirm the role of eNOS in NO-dependent Ras activation, we compared the responses to stimulation with CD3 Ab of T lymphoblasts from eNOS knockout and wild-type mice (Fig. 2 *E* and *F*). Ras activation in eNOS-deficient cells was lower than in wild-type cells and was increased by treatment with the NO donor DETA-NO (Fig. 2*F* and Fig. S3*E*). These results demonstrate that eNOS-derived NO positively regulates Ras/ERK signaling in response to antigen-specific T cell–APC interactions.

eNOS Preferentially Activates N-Ras in Antigen-Stimulated T Cells. To identify the Ras isoform(s) activated by eNOS, we used isoform-

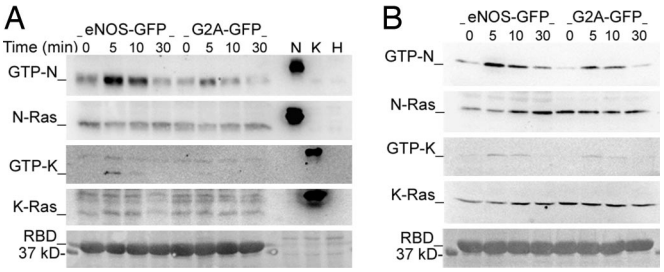

Fig. 3. eNOS selectively activates N-Ras in antigen-stimulated T cells. (*A*) Time course activation of endogenous N- and K-Ras in eNOS- and G2A-GFP cells stimulated with CD3 Ab. Extracts of cells expressing HA-tagged N-, H-, and K-Ras were loaded as controls of antibody specificity. (*B*) eNOS- and G2A-GFP cells transiently expressing CFP-N-Ras or -K-Ras were stimulated with SEB-pulsed Raji APC for the times indicated. The expression of activated and total Ras was analyzed as in *A*. The loadings of GST-RBD-Raf-1 (RBD) are also shown. Each panel is representative of three independent experiments.

specific anti-Ras antibodies. Endogenous N-Ras was activated in response to TCR engagement, and this activation was markedly increased in eNOS-GFP cells (Fig. 3*A* and Fig. S4*A*). In contrast, activation of K-Ras was barely detected, although a very slight increase was observed in eNOS-GFP cells (Fig. 3*A* and Fig. S4*B*). H-Ras was not detected even in whole-cell extracts (Fig. S5*A*). Similar results were obtained by transfecting cells with constructs encoding enhanced cyan fluorescent protein (CFP) linked to N- or K-Ras (CFP-N-Ras and -K-Ras) and stimulating with SEB-pulsed Raji APC (Fig. 3*B* and Fig. S4 *C* and *D*). These results demonstrate that eNOS-derived NO preferentially activates N-Ras in superantigen-specific T cell–APC conjugates. However, it is worth noting that exogenously expressed H-Ras behaved in a way similar to N-Ras (Fig. S5*B*).

eNOS Activates N-Ras on the Golgi Complex. Because H- and N-Ras, but not K-Ras, are variably localized on the Golgi (16, 17), we examined whether eNOS underlies the preferential activation of N-Ras in this cell compartment. We performed triple fluorescence confocal microscopy analysis of stable conjugates formed between SEB-pulsed Raji APC and eNOS-GFP or G2A-GFP cells cotransfected with enhanced yellow fluorescent protein (YFP)-RBD-Raf-1 and CFP-N-Ras or -K-Ras (Fig. 4). N-Ras and RBD-Raf-1 colocalized predominantly with eNOS on the Golgi of T cells, whereas K-Ras showed a limited colocalization with RBD-Raf-1 at the plasma membrane (Fig. 4*A*). More detailed analysis showed that the localizations of N-Ras on the Golgi and K-Ras at the plasma membrane change little upon stimulation with SEB-pulsed APC (Fig. 4*B*). In contrast, the localization of RBD-Raf-1 on the Golgi of N-Ras-transfected cells increased, and this effect was greater in eNOS-GFP than in G2A-GFP cells (78.7% cells vs. 54.8% cells) (Fig. 4*B*). Small amounts of RBD-Raf-1 were detected at the plasma membrane of SEB-stimulated eNOS- and G2A-GFP cells expressing CFP-K-Ras (21.0% and 10.0%, respectively) (Fig. 4*B*).

To investigate the dynamics of eNOS-mediated activation of N-Ras on the Golgi, we performed time lapse confocal fluorescence videomicroscopy of YFP-RBD-Raf-1 and CFP-N-Ras in SEB-stimulated eNOS-GFP T cells (Fig. 4 *C* and *D*). Initially, RBD-Raf-1 was broadly localized in the cytoplasm, whereas N-Ras was concentrated with eNOS-GFP on the Golgi (Fig. 4*C*). In response to SEB stimulation, RBD-Raf-1 progressively redistributed to the Golgi, colocalizing with N-Ras and eNOS-GFP after ≈4 min (Fig. 4*C*). Interestingly, although the localization of RBD-Raf-1 on the Golgi was 2-fold higher in eNOS-GFP than in G2A-GFP cells, the kinetic constants of redistribution were similar (2.30 ± 0.5 and 2.07 ± 0.4, respectively) (Fig. 4*D*). Because only the activated form of Ras can recruit Raf-1 (16), these data indicate that

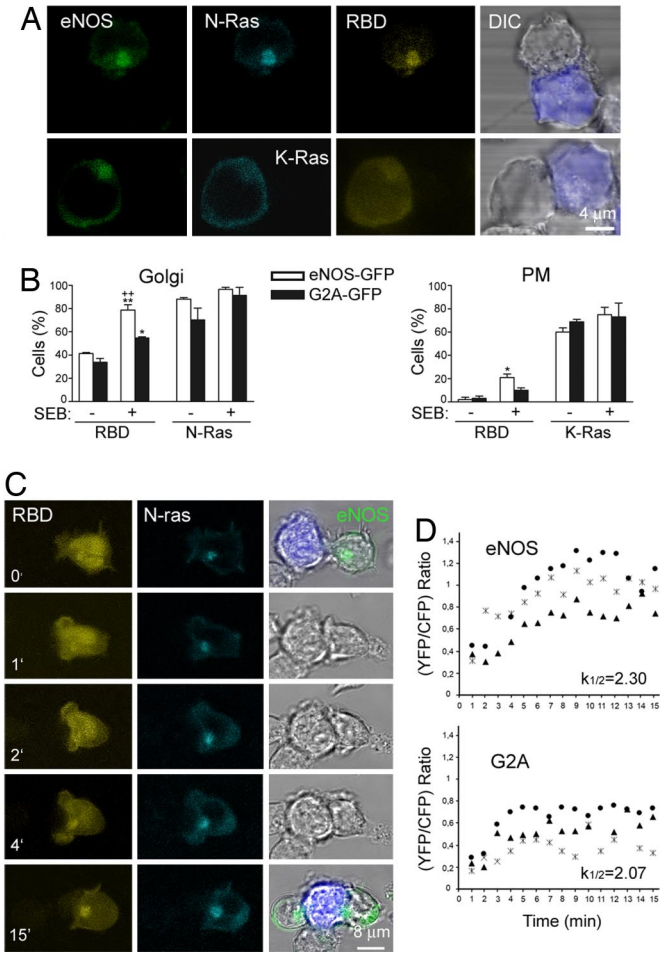

Fig. 4. eNOS activates N-Ras on the Golgi complex of APC-conjugated T cells. (*A*) SEB-pulsed Raji APC were mixed with eNOS-GFP cells cotransfected with YFP-RBD-Raf-1 (RBD) and CFP-N-Ras (*Upper*) or -K-Ras (*Lower*). The subcellular localizations of eNOS (green), Ras (cyan), and RBD-Raf-1 (yellow) are shown. Raji APC (blue) was superposed on DIC images. (*B*) Quantitative analysis of the cellular localization of YFP-RBD-Raf-1 (RBD) in T cell–APC conjugates between naive (−) or SEB-pulsed (+) Raji APC and eNOS- or G2A-GFP cells expressing YFP-RBD-RAF-1 and CFP-N-Ras (*Left*) or -K-Ras (*Right*). Histograms show the percentages of T cells showing accumulation of YFP-RBD-Raf-1 and CFP-N-Ras on the Golgi (*Left*) or CFP-K-Ras at the plasma membrane (PM) (*Right*). More than 100 cells were scored for each condition. Data are the means ± SEM of three independent experiments. **, $P \leq 0.001$; *, $P \leq 0.05$ compared with nonstimulated cells; ++, $P \leq 0.001$ compared with SEB-stimulated G2A-GFP cells. (*C*) eNOS-GFP cells transiently cotransfected with YFP-RBD-Raf-1 (yellow) and CFP-N-Ras (cyan) were mixed with SEB-pulsed Raji APC, and images were recorded by real-time confocal fluorescence microscopy at the times indicated. The fluorescence signals of eNOS (green at 0 and 15 min) and Raji APC (blue) were superposed on DIC images. (*D*) T cells cotransfected with CFP-N-Ras and YFP-RBD-Raf-1 were activated as in *C*, and the redistribution of RBD-Raf-1 toward CFP-N-Ras on the Golgi was monitored from the time of initial intercellular contacts. Three representative traces and the mean kinetic constants of YFP-RBD-Raf-1 redistribution are presented for each condition.

eNOS activates N-Ras on the Golgi without modifying the kinetics of Raf-1 redistribution.

Activated eNOS *S*-Nitrosylates Proteins on the Golgi Complex of Antigen-Stimulated T Cells. We next studied the localization of activated eNOS (eNOS-pSer^{1179}) in APC-conjugated T cells expressing CFP-N-Ras or -K-Ras (Fig. 5*A*). Phosphorylated eNOS colocalized mainly with N-Ras on the Golgi and partially with K-Ras at some points of the plasma membrane that are in contact with APC (Fig. 5*A*). In contrast, phospho-eNOS was barely de-

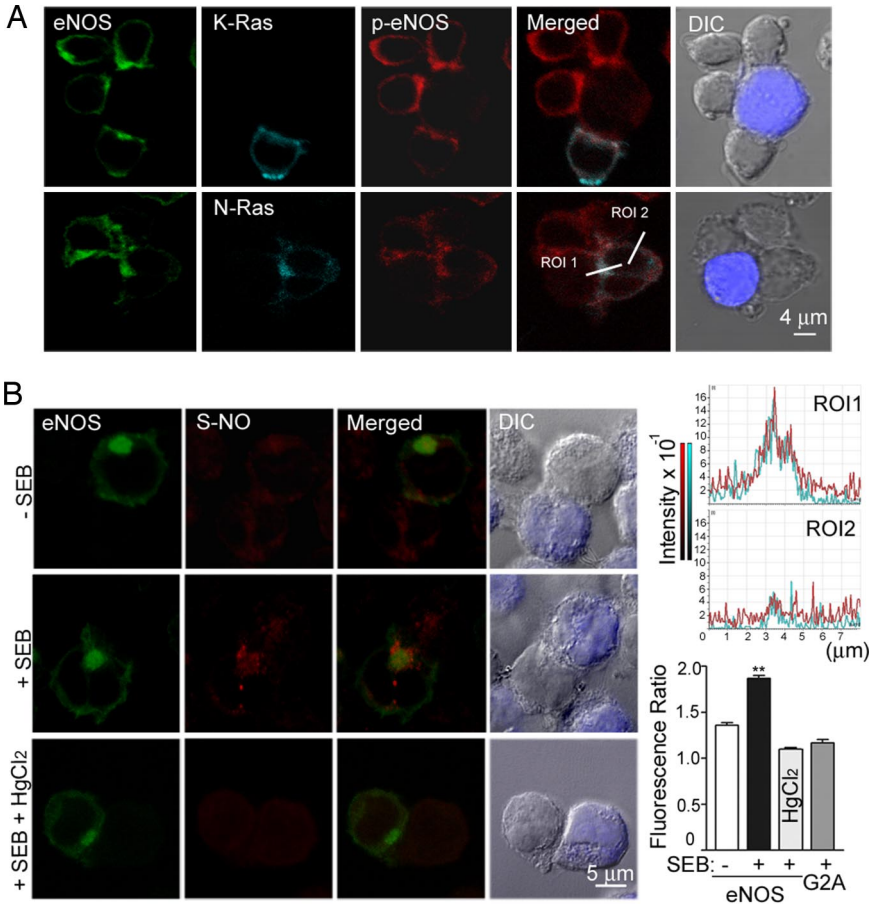

Fig. 5. Activated eNOS *S*-nitrosylates proteins on the Golgi complex of APC-conjugated T cells. (*A*) eNOS-GFP cells expressing CFP-K-Ras or -N-Ras were mixed with SEB-pulsed Raji APC for 10 min. Cells were fixed and then stained with eNOS-pSer^{1179} pAb. The localization of phospho-eNOS (red), eNOS (green), and Ras (cyan) were analyzed by confocal fluorescence microscopy. The figure shows merged images of *p*-eNOS with CFP-N-Ras and -K-Ras, and fluorescence profile analysis of the intensity and distribution *p*-eNOS (red) and CFP-N-Ras (blue) along an 8-μm cross-section through the region of interest (ROI) (*Bottom Right*). ROI1, the Golgi; ROI2, the plasma membrane. (*B*) (*Left*) eNOS-GFP (green) cells were mixed with naive (−) or SEB-pulsed (+) Raji APC, and *S*-nitrosylation of endogenous proteins (red) was detected with anti-*S*-nitrosocysteine mAb. To control for specificity, paraformaldehyde-fixed conjugates were treated before *S*-nitrosocysteine staining with 0.2% $HgCl_2$ to break protein *S*—NO bonds. Raji APC (blue) was superposed on DIC images. (*Right*) The corresponding Golgi/cytoplasm polarization ratios of *S*-nitrosocysteine staining, including SEB-stimulated G2A-GFP cells, are represented as means ± SEM of three independent experiments. More than 80 cells were scored. **, $P \leq 0.001$ compared with non-stimulated cells.

tected in G2A-GFP cells (Fig. S6). To explore whether eNOS could mediate local *S*-nitrosylation of proteins on the Golgi, we examined protein *S*-nitrosylation in APC-conjugated T cells by immunofluoresence analysis with a nitrosocysteine-specific antibody (Fig. 5*B*). Whereas SEB-pulsed APC induced a 1.87-fold increase in *S*-nitrosocysteine polarization at the proximity of eNOS-GFP, polarized *S*-nitrosocysteine staining did not increase in G2A-GFP cells (Fig. 5*B*). The SEB-induced pattern of protein *S*-nitrosylation in eNOS-GFP cells was abolished by $HgCl_2$ pretreatment (Fig. 5*B*). These results suggest that during antigen-specific T cell–APC interactions the activation of eNOS leads to protein *S*-nitrosylation on the Golgi.

eNOS Activates N-Ras by *S*-Nitrosylation at Cys^{118}. To study whether Ras was among the *S*-nitrosylated proteins detected by immunofluorescence, we performed biotin switch assays (21). CD3 stimulation significantly increased *S*-nitrosylation of Ras in eNOS- but not in G2A-GFP cells (Fig. 6*A*, and Fig. S7*A*). NO from donors is known to *S*-nitrosylate H-Ras on Cys^{118}, and this modification increases the proportion of active GTP-bound H-Ras by promoting GDP–GTP exchange (11). We therefore studied whether TCR engagement would induce eNOS-mediated *S*-nitrosylation of N-Ras on Cys^{118}; we found that stimulation of eNOS-GFP cells with CD3 Ab or DEA-NO induced *S*-nitrosylation of wild-type N-Ras but had little detectable effect on *S*-nitrosylation of C118S N-Ras (Fig. 6*B* and Fig. S7*B*).

To investigate whether Cys^{118} is critical for NO-dependent Ras activation, we transfected CH7C17 T cells with wild-type or C118S CFP-Ras isoforms and stimulated with CD3 Ab in the absence or presence of DETA-NO. Whereas DETA-NO activated all wild-type Ras isoforms to a similar extent, only N- and H-Ras were noticeably activated in response to CD3 Ab (Fig. 6*C* and Figs. S8 *A* and *B* and S9*A*). The C118S mutation strongly reduced the activation of Ras; however, a very low activation in response to CD3 Ab was still detected (Fig. 6*C* and Figs. S8 *A* and *B* and S9*A*), suggesting that an NO-independent component may be also required for Ras activation. To study whether the C118S mutation also impaired Ras activation by NO derived from eNOS, we stimulated eNOS-GFP cells transiently expressing C118S Ras mutants with CD3 Ab and determined Ras activation as above. Whereas wild-type N- and H-Ras were clearly activated in eNOS-GFP cells, activation of their corresponding C118S mutants was weak, similar to wild-type activation in G2A-GFP cells (Fig. 6*D* and Figs. S8*C* and S9*B*). In contrast, activation of wild-type K-Ras was weak in both cell types and similar to C118S Ras (Fig. 6*D* and Fig. S8*D*). These results indicate that eNOS *S*-nitrosylates N-Ras at Cys^{118} upon TCR engagement; moreover, even though this residue is important for NO-dependent activation of all three Ras isoforms, only N- and H-Ras were clearly activated by eNOS-derived NO in TCR-stimulated T cells.

Cys^{118} Is Dispensable for Localization but Critical for eNOS-Mediated N-Ras Activation and Function on the Golgi. Impaired activation of C118S Ras mutants was not caused by mislocalization because they are localized similarly to their wild-type counterparts (Fig. S10). To explore whether eNOS-mediated *S*-nitrosylation of Cys^{118} activates N-Ras on the Golgi, we formed stable conjugates between SEB-pulsed Raji APC and eNOS-GFP cells cotransfected with YFP-RBD-Raf-1 and wild-type or C118S CFP-N-Ras and analyzed RBD-Raf-1 localization as in Fig. 4*B*. Antigen stimulation increased Golgi redistribution of Raf-1 in both cases, but the proportion of Golgi-redistributed RBD-Raf-1 was considerably higher in cells expressing wild-type N-Ras than in cells expressing the C118S mutant (85.0% vs. 56.0%) (Fig. 6*E*). In contrast, in cells

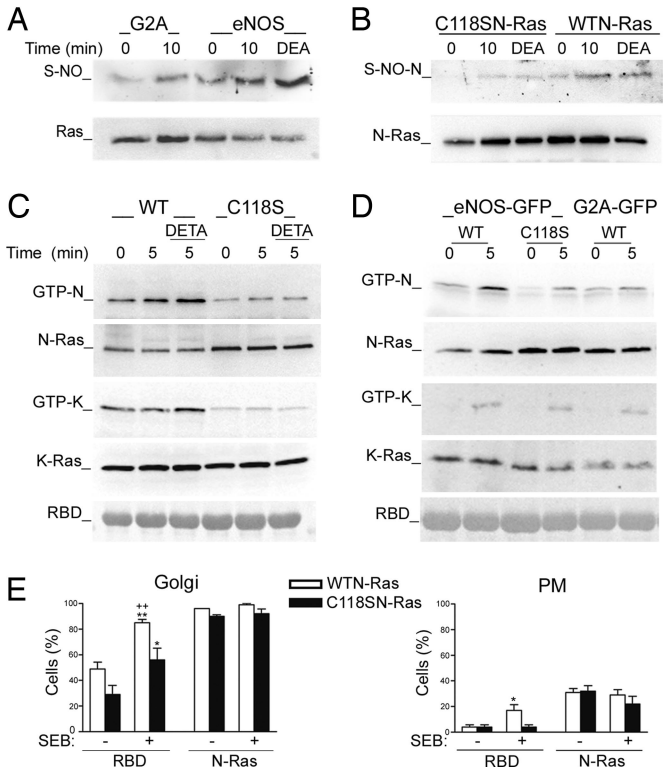

Fig. 6. eNOS activates N-Ras on the Golgi complex by *S*-nitrosylation of Cys^{118}. (*A*) Biotin switch of endogenous Ras *S*-nitrosylation in eNOS- and G2A-GFP cells stimulated with CD3 Ab as indicated or 1 mM DEA-NO (DEA) for 15 min. (*B*) eNOS-GFP cells expressing wild-type or C118S HA-N-Ras were stimulated as in *A*. Cell extracts were analyzed by biotin switch and immunoblot with anti-Ras Ab. (*C*) CH7C17 T cells transfected with wild-type or C118S CFP-N-Ras or -K-Ras were stimulated with CD3 Ab for the times indicated in the presence or absence of DETA-NO (DETA). Ras activation was detected by GST-RBD-Raf-1 pull-down assay. (*D*) eNOS- and G2A-GFP cells expressing wild-type CFP-N-Ras or -K-Ras, and eNOS-GFP cells expressing the corresponding C118S mutant, were stimulated with CD3 Ab; the activation of Ras was determined as in *C*. Controls GST-RBD-Raf-1 (RBD) are shown. Each panel is representative of at least three independent experiments. (*E*) eNOS-GFP cells coexpressing YFP-RBD-Raf-1 (RBD) and wild-type or C118S CFP-N-Ras were mixed with naive (−) or SEB-pulsed (+) Raji APC. Histograms show the percentages of cells showing accumulations of YFP-RBD-Raf-1 and wild-type or C118S N-Ras on the Golgi (*Left*) or the plasma membrane (PM) (*Right*). More than 100 cells were scored for each condition. Data are means ± SEM of three independent experiments. **, $P \leq 0.001$ and *, $P \leq 0.05$ compared with nonstimulated cells; ++, $P \leq 0.001$ compared with SEB-stimulated C118S N-Ras-expressing cells.

expressing wild-type N-Ras the proportion of RBD-Raf-1 at the plasma membrane was low (17%) although slightly higher than in cells expressing C118S N-Ras (4%) (Fig. 6*E*).

To assess the functional relevance of N-Ras *S*-nitrosylation in T cells, we determined the extent of activation-induced programmed cell death, which can be detected by the binding of annexin V on the plasma membrane as a marker of phosphatydilserine externalization (Fig. S11). Transfection of wild-type but not C118S N-Ras increased the binding of annexin V to CD3-stimulated eNOS-GFP cells (Fig. S11). Taken together, these results strongly suggest that during T cell activation, eNOS selectively activates N-Ras on the Golgi complex and regulates T cell apoptosis by *S*-nitrosylation on Cys^{118}.

Discussion

In this work we have shown that the regulation of Ras/ERK signaling in antigen-stimulated T cells is compartmentalized by the local production of NO. eNOS positively regulates Ras activation during antigen-specific T cell–APC interactions by *S*-nitrosylation on the Golgi, thus favoring activation-induced T cell death. eNOS-derived NO preferentially activates N-Ras but not K-Ras even when this isoform of Ras is overexpressed. In contrast, when expressed in T cells, H-Ras is activated to a similar extent as N-Ras, suggesting the presence of common eNOS-dependent regulatory elements on both isoforms.

The different compartmentalization of the known Ras isoforms in cellular endomembranes is critical for their specific biological activities. Our results show that in superantigen-specific T cell–APC conjugates N-Ras colocalizes with phosphorylated eNOS on the Golgi, where it is strongly activated in response to TCR engagement, as indicated by the redistribution of RBD-Raf-1 toward this organelle. In contrast, K-Ras was preferentially concentrated at the plasma membrane, where it is activated only slightly. We have also shown that the kinetic of RBD-Raf-1 redistribution was unaffected by eNOS, even though eNOS-derived NO rapidly increased the TCR-dependent activation of N-Ras on the Golgi. Previous studies have shown that whereas K-Ras is constitutively localized at the plasma membrane under steady-state conditions, depalmitoylation–palmitoylation cycling drives a rapid exchange of H- and N-Ras between the plasma membrane and the Golgi (16, 17). eNOS also traffics between these cell compartments, displaying substantial Golgi localization as a consequence of its inefficient acylation (17, 22, 23). In this context, our results demonstrate that eNOS selectively activates N-Ras on the Golgi, although we cannot completely rule out the possibility that the minor fraction of eNOS associated with the plasma membrane might play a role in the slight activation of K-Ras we detected.

Whether activation of Ras by tyrosine kinase-coupled receptors takes place on Golgi or at the plasma membrane is still a matter of open debate. Some groups, using new RBD-based specific probes, have detected Ras activation preferentially at the plasma membrane (24, 25). However, studies carried out using classical fluorescent RBD probes to detect the subcellular activation of Ras in T cells have shown that TCR engagement or CD28 costimulation activate H- and N-Ras almost exclusively on the Golgi, whereas costimulation via the integrin LFA-1 activates Ras on both the Golgi and the plasma membrane (26). In light of this finding, our results suggest that the release of NO from eNOS might provide a link between CD28 costimulation and the activation of N-Ras on the Golgi. In fact, CD28 costimulation increases the production of NO in T cells and is responsible for the major part of sustained Ca^{2+} fluxing and activation of PI3-K (3), two key signaling pathways upstream of the activation of eNOS (6, 10).

Recent studies have shown *S*-nitrosylation to be an important molecular mechanism in NO-dependent signal transduction (27, 28). We have demonstrated here that eNOS increases *S*-nitrosylation of proteins on the Golgi of superantigen-activated T cells and nitrosylated N-Ras on Cys^{118}. Moreover, although Cys^{118} is a key amino acid for the activation of N-, H-, and K-Ras by NO from donors, our experiments indicate that, upon TCR engagement, eNOS is able to activate only N-Ras and H-Ras. Because the C118S mutant was significantly less activated than wild-type N-Ras, despite maintaining its normal localization on the Golgi, our results strongly suggest that eNOS *S*-nitrosylates N-Ras in this organelle. Our findings are in agreement with previous work demonstrating that the local production of eNOS-derived NO on the Golgi can regulate *S*-nitrosylation-dependent protein activity (29).

The existence of eNOS-mediated N-Ras *S*-nitrosylation on the Golgi is compatible with a mechanism in which NO facilitates GDP–GTP exchange (30); this model proposes that *S*-nitrosylation may be involved in the generation and quenching of Cys radicals that weaken the interaction of Ras with GDP and enhance the binding of GTP. Thus, it is feasible that, in response to antigen-binding to the TCR, simultaneous PI3K-Akt and PLC-γ-Ca^{2+} signals activate Golgi-localized eNOS by phosphorylation on Ser^{1179} and Ca^{2+} binding to calmodulin, respectively (10). eNOS-

derived NO would then activate N-Ras by enhancing guanine nucleotide exchange.

Controversies exist about the functional role of NO-mediated *S*-nitrosylation in Ras signaling. Inhibition of ERK activation by *S*-nitrosylation of H-Ras has been reported in human embryonic kidney 293 cells transfected with nNOS (31), whereas in T lymphocytes and neurons *S*-nitrosylation is associated with activation of this pathway (12, 32). In this regard, parallels can be drawn between the mechanisms of action of NO in neurons and those described here in T cells. The binding of *N*-methyl-D-aspartate (NMDA) to its receptor on neurons stimulates neuronal NOS to produce NO, which *S*-nitrosylates the small GTPases Ras and Dexras, located in membrane-associated complexes with cell-specific adaptor and scaffolding proteins (33). Whether the association of eNOS with similar protein complexes on the Golgi of antigen-stimulated T cells is important for TCR-induced N-Ras *S*-nitrosylation and activation merits further investigation.

In summary, our data provide insights into the regulation of Ras/ERK activation by defining an eNOS-dependent mechanism that allows differential activation of Ras isoforms at specific subcellular compartments in T cells. In this regard, it has been reported that $CD8^+$ selection is impaired in immature thymocytes from N-Ras knockout mice (34) and that activation of Ras/ERK signaling on the plasma membrane or the Golgi regulates cell fate decisions in a mouse model of T cell development (35). In this model, activation of Ras on the Golgi directs positive selection, whereas activation on the plasma membrane directs negative selection depending on the TCR–antigen affinity. Our finding that, in response to strong TCR engagement, N-Ras *S*-nitrosylation positively regulates activation-induced cell death in mature T cells also argues in favor of a functional compartmentalization of Ras. Whether eNOS underlies the role of N-Ras in thymic selection deserves further investigation.

Materials and Methods

Further information is presented in *SI Material and Methods*.

Cell Transfection Studies and Cell Sorting. T cells (15×10^6) were transfected by using the Pulser X-cell Electroporation System (Bio-Rad) at 250 V and 1,200 μF with 25 μg of expression plasmids encoding the indicated constructs. T cells stably expressing GFP, eNOS-GFP, or G2A-GFP were obtained by cell sorting with a MoFlo flow cytometer (DakoCytomation).

T Cell Activation and Raf-Ras-Binding Domain Pull-Down. T cells (15×10^6) were serum-starved at 37°C for 2 h before stimulation with CD3 T3b mAb (5 μg/ml), and after 2 min goat anti-mouse IgG (10 μg/ml) was added as cross-linker for 30 min. For superantigen-specific stimulation, APCs (5×10^6) were incubated with SEB (0.5 μg/ml) for 30 min and then mixed with T cells at a ratio of 1:3. For antigen-specific stimulation, HOM-2 APCs (5×10^6) were incubated at 37°C for 3 h with 200 μg/ml HA 307–319 peptide and then mixed with T cells at a ratio of 1:3.

To detect GTP-bound Ras, cells were sedimented and lysed in buffer containing [150 mM NaCl, 25 mM Hepes, 10 mM $MgCl_2$,10% (vol/vol) glycerol, 1% Nonidet P-40, 50 μM GTP, 1 mM Na_3VO_4, 25 mM NaF] and protease inhibitors (Complete; Roche Molecular Biochemicals) at 4°C. Lysates were cleared by centrifugation and incubated (60 min, 4°C) with GST-Raf-1-RBD fusion proteins coupled to glutathione–Sepharose beads (Amersham Biosciences). After incubation, GTP-bound Ras was eluted with Laemmli sample buffer, and samples were separated by 15% SDS/PAGE in parallel with corresponding whole-cell lysates to detect GTP-bound and total Ras.

Time-Lapse Fluorescence Microscopy. Cell conjugates in phenol red-free RPMI medium 1640 containing 25 mM Hepes and 2% FBS were allowed to settle in LabTek II chambers (Nalge Nunc International) and maintained at 37°C in a 5% CO_2 atmosphere in an incubator coupled to a Leica TCS SP2 confocal microscope. Time lapse confocal images were collected with an HCX PL APO 40× NA 1.32 oil-immersion objective lens (Leica). T cells transiently cotransfected with YFP-RBD-Raf-1 and either CFP-N-Ras or -K-Ras were mixed with SEB-pulsed-APC, and fluorescence and differential interference contrast (DIC) images were captured every 1 min. Six confocal Z-sections were necessary to capture the entire fluorescent signal at each time.

ACKNOWLEDGMENTS. We thank Dr. E. O'Connor, A. Álvarez-Barrientos, and A. Martínez for assistance with flow cytometry. We also thank Dr. S. Lamas for critical readings and Dr. S. Bartlett for editorial assistance. This work was supported by Fondo de Investigaciones (FIS) Grants PI070356 and Contrato-Investigador FIS CP02/23024 (to J.M.S.), BFU2005-08435/BMC (to F.S.M.), SAF2006-04247 and BM04/179-02 (Fundació "la Caixa") (to J.M.R.), SAF2005-01366 (to J.V.E.), and Contrato-Investigador FIS CP07/00171 (to V.M.V.) and CP07/00143 (to A.M.-R.). S.I., A.P.-R., and C.A.G.-D. were recipients of fellowships from Centro Nacional de Investigaciones Cardiovasculares (CNIC)-Bancaja, Comunidad Autonoma de Madrid, and Instituto de Salud Carlos III (ISCIII), respectively.

1. Bogdan C (2001) Nitric oxide and the immune response. *Nat Immunol* 2:907–916.
2. Beltran B, *et al.* (2002) Inhibition of mitochondrial respiration by endogenous nitric oxide: A critical step in Fas signaling. *Proc Natl Acad Sci USA* 99:8892–8897.
3. Nagy G, Koncz A, Perl A (2003) T cell activation-induced mitochondrial hyperpolarization is mediated by Ca^{2+}- and redox-dependent production of nitric oxide. *J Immunol* 171:5188–5197.
4. Reiling N, *et al.* (1996) Nitric oxide synthase: Expression of the endothelial, Ca^{2+}/calmodulin-dependent isoform in human B and T lymphocytes. *Eur J Immunol* 26:511–516.
5. Dimmeler S, *et al.* (1999) Activation of nitric oxide synthase in endothelial cells by Akt-dependent phosphorylation. *Nature* 399:601–605.
6. Fulton D, *et al.* (1999) Regulation of endothelium-derived nitric oxide production by the protein kinase Akt. *Nature* 399:597–601.
7. Erwin PA, Mitchell DA, Sartoretto J, Marletta MA, Michel T (2006) Subcellular targeting and differential *S*-nitrosylation of endothelial nitric-oxide synthase. *J Biol Chem* 281:151–157.
8. Erwin PA, Lin AJ, Golan DE, Michel T (2005) Receptor-regulated dynamic *S*-nitrosylation of endothelial nitric-oxide synthase in vascular endothelial cells. *J Biol Chem* 280:19888–19894.
9. Liu J, Hughes TE, Sessa WC (1997) The first 35 amino acids and fatty acylation sites determine the molecular targeting of endothelial nitric oxide synthase into the Golgi region of cells: A green fluorescent protein study. *J Cell Biol* 137:1525–1535.
10. Ibiza S, *et al.* (2006) Endothelial nitric oxide synthase regulates T cell receptor signaling at the immunological synapse. *Immunity* 24:753–765.
11. Lander HM, *et al.* (1997) A molecular redox switch on p21(ras): Structural basis for the nitric oxide–p21(ras) interaction. *J Biol Chem* 272:4323–4326.
12. Lander HM, Jacovina AT, Davis RJ, Tauras JM (1996) Differential activation of mitogen-activated protein kinases by nitric oxide-related species. *J Biol Chem* 271:19705–19709.
13. Genot E, Cantrell DA (2000) Ras regulation and function in lymphocytes. *Curr Opin Immunol* 12:289–294.
14. Downward J, Graves JD, Warne PH, Rayter S, Cantrell DA (1990) Stimulation of p21ras upon T-cell activation. *Nature* 346:719–723.
15. Perez de Castro I, Bivona TG, Philips MR, Pellicer A (2004) Ras activation in Jurkat T cells following low-grade stimulation of the T-cell receptor is specific to N-Ras and occurs only on the Golgi apparatus. *Mol Cell Biol* 24:3485–3496.
16. Mor A, Philips MR (2006) Compartmentalized Ras/MAPK signaling. *Annu Rev Immunol* 24:771–800.
17. Rocks O, *et al.* (2005) An acylation cycle regulates localization and activity of palmitoylated Ras isoforms. *Science* 307:1746–1752.
18. Dong C, Davis RJ, Flavell RA (2002) MAP kinases in the immune response. *Annu Rev Immunol* 20:55–72.
19. Bivona TG, *et al.* (2003) Phospholipase Cγ activates Ras on the Golgi apparatus by means of Ras-GRP1. *Nature* 424:694–698.
20. Gonzalez E, Kou R, Lin AJ, Golan DE, Michel T (2002) Subcellular targeting and agonist-induced site-specific phosphorylation of endothelial nitric-oxide synthase. *J Biol Chem* 277:39554–39560.
21. Jaffrey SR, Erdjument-Bromage H, Ferris CD, Tempst P, Snyder SH (2001) Protein *S*-nitrosylation: A physiological signal for neuronal nitric oxide. *Nat Cell Biol* 3:193–197.
22. Fernandez-Hernando C, *et al.* (2006) Identification of Golgi-localized acyl transferases that palmitoylate and regulate endothelial nitric oxide synthase. *J Cell Biol* 174:369–377.
23. Dudzinski DM, Michel T (2007) Life history of eNOS: Partners and pathways. *Cardiovasc Res* 75:247–260.
24. Mochizuki N, *et al.* (2001) Spatio-temporal images of growth factor-induced activation of Ras and Rap1. *Nature* 411:1065–1068.
25. Augsten M, *et al.* (2006) Live-cell imaging of endogenous Ras-GTP illustrates predominant Ras activation at the plasma membrane. *EMBO Rep* 7:46–51.
26. Mor A, *et al.* (2007) The lymphocyte function-associated antigen-1 receptor costimulates plasma membrane Ras via phospholipase D2. *Nat Cell Biol* 9:713–719.
27. Martinez-Ruiz A, *et al.* (2005) *S*-nitrosylation of Hsp90 promotes the inhibition of its ATPase and endothelial nitric oxide synthase regulatory activities. *Proc Natl Acad Sci USA* 102:8525–8530.
28. Whalen EJ, *et al.* (2007) Regulation of β-adrenergic receptor signaling by *S*-nitrosylation of G protein-coupled receptor kinase 2. *Cell* 129:511–522.
29. Iwakiri Y, *et al.* (2006) Nitric oxide synthase generates nitric oxide locally to regulate compartmentalized protein *S*-nitrosylation and protein trafficking. *Proc Natl Acad Sci USA* 103:19777–19782.
30. Raines KW, Bonini MG, Campbell SL (2007) Nitric oxide cell signaling: *S*-nitrosylation of Ras superfamily GTPases. *Cardiovasc Res* 75:229–239.
31. Raines KW, *et al.* (2004) Nitric oxide inhibition of ERK1/2 activity in cells expressing neuronal nitric-oxide synthase. *J Biol Chem* 279:3933–3940.
32. Yun HY, Gonzalez-Zulueta M, Dawson VL, Dawson TM (1998) Nitric oxide mediates *N*-methyl-D-aspartate receptor-induced activation of p21ras. *Proc Natl Acad Sci USA* 95:5773–5778.
33. Cheah JH, *et al.* (2006) NMDA receptor-nitric oxide transmission mediates neuronal iron homeostasis via the GTPase Dexras1. *Neuron* 51:431–440.
34. Perez de Castro I, *et al.* (2003) Mice deficient for N-ras: Impaired antiviral immune response and T-cell function. *Cancer Res* 63:1615–1622.
35. Daniels MA, *et al.* (2006) Thymic selection threshold defined by compartmentalization of Ras/MAPK signalling. *Nature* 444:724–729.